Proceedings of the ASME 2010 International Design Engineering Technical Conferences & Computers and Information in Engineering Conference
IDETC/CIE 2010
August 15-18, 2010, Montreal, Quebec, Canada

DETC2010-28491

DEXTEROUS WORKSPACE OF N-PRRR PLANAR PARALLEL MANIPULATORS

André Gallant Email: eag3440@umoncton.ca

Roger Boudreau* Email: roger.a.boudreau@umoncton.ca

Marise Gallant Email: marise.gallant@umoncton.ca

Département de génie mécanique
Université de Moncton
Moncton, New Brunswick, E1A 3E9
Canada

ABSTRACT

In this work, a method is presented to geometrically determine the dexterous workspace boundary of kinematically redundant n-PRRR[1] planar parallel manipulators. The dexterous workspace of each non-redundant RRR kinematic chain is first determined using a four-bar mechanism analogy. The effect of the prismatic actuator is then considered to yield the workspace of each PRRR kinematic chain. The intersection of the dexterous workspaces of all the kinematic chains is then obtained to determine the dexterous workspace of the planar n-PRRR manipulator. The Gauss Divergence Theorem applied to planar surfaces is implemented to compute the total dexterous workspace area. Finally, two examples are shown to demonstrate applications of the method.

INTRODUCTION

The shape and size of the dexterous workspace can be used to evaluate and to compare the dimensions of a given architecture or to compare different architectures. The dexterous workspace can be defined as the volume where the end-effector (tool) of a manipulator is able to reach with any orientation. Thus, for planar manipulators, any position where the end-effector can complete a full revolution is part of the dexterous workspace.

Several researchers have studied the dexterous as well as other types of workspaces for the non-redundant 3-RRR symmetric planar architecture [1–3]. The dexterous workspace in these works was defined by a maximum of two concentric circles for each of the three kinematic chains. Geometric methods for the dexterous workspace of non-symmetric 3-RRR manipulators have been developped [4, 5]. Again, two concentric circles for the dexterous workspace per kinematic chain were identified. For the 3-RRR architecture, a dexterous workspace of two concentric circles per chain can be called the controllably dexterous workspace where the dexterous workspace is devoid of discontinuities [3]. Zhaohui and Zhonghe [6] identified a third concentric circle near the base of each kinematic chain by using the four-bar mechanism analogy on a symmetric 3-RRR manipulator. Work has also been done to determine various workspaces of planar parallel manipulators with joint limits [7]. Hay and Snyman [8] developed a method to map the boundary of the workspace of planar parallel manipulators which they named the chord method.

Several works have used an integration of the workspace boundary based on the Gauss Divergence Theorem [9] to obtain its surface area [1, 7, 10].

Parallel manipulators have certain advantages over their serial counterparts such as higher payload capacities. However, they suffer from a reduced workspace that generally contains

*Address all correspondence to this author.

[1]The notation n-PRRR indicates that the manipulator consists of *n* serial kinematic chains that connect the base to the end-effector. Each chain is composed of two actuated (therefore underlined) joints and two passive revolute joints. P indicates a prismatic joint while R indicates a revolute joint.

many singularities. To counterbalance this, Ebrahimi et al. [11] introduced kinematic redundancy by adding a prismatic actuator to the base of each kinematic chain of the 3-RRR manipulator. The effects of the redundancy on the workspace and on the presence of singularities were determined. The dexterous workspace was obtained with a discreet method which is computationally inefficient and does not yield an exact solution.

The dexterous workspace of more general versions of the planar 3-PRRR architecture, the planar n-PRRR architectures, are the subject of this work. A methodology using a four-bar mechanism analogy to determine the dexterous workspace of 3-PRRR manipulators geometrically was presented in [12]. The present paper provides details for implementing this method which is valid for any planar n-PRRR manipulator.

The architecture of kinematically redundant n-PRRR planar parallel manipulators is first presented. The method to determine the workspace of n-PRRR manipulators is then explained. Two examples of n-PRRR manipulators are presented in order to illustrate applications of the method.

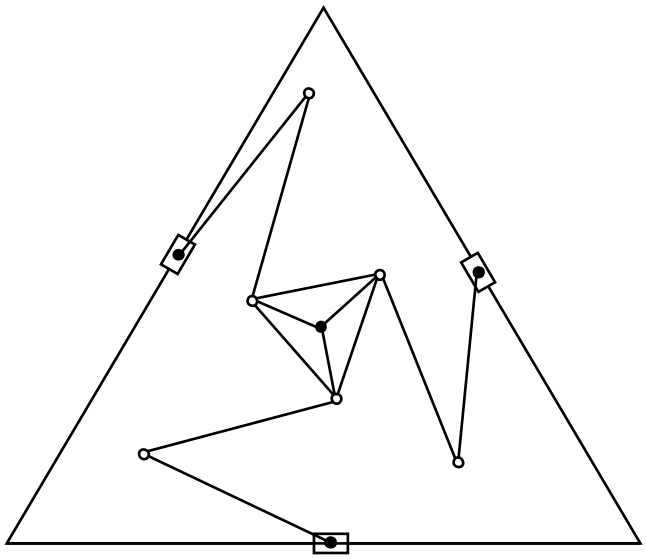

Figure 1. Example 3-PRRR planar parallel manipulator

ARCHITECTURE

An example 3-PRRR manipulator is shown in Figure 1. In this figure, it can be seen that the base of each kinematic chain of a 3-RRR manipulator is attached to a prismatic actuator to form a 3-PRRR manipulator. Although Figure 1 shows a 3-PRRR manipulator with the prismatic actuators forming a triangle, the prismatic actuators of n-PRRR manipulators can be configured in any arrangement and there can be any number of kinematic chains. The process of determining the dexterous workspace of all planar n-PRRR architectures is essentially the same. Since only the dexterous workspace is studied, the term workspace will henceforth be used to refer to the dexterous workspace.

METHODOLOGY

The method for determining the workspace of n-PRRR planar parallel manipulators as well as its area can be summarized by the following steps:

1. Determine the geometry of the workspace of each kinematic chain.
2. Determine the points of intersection of each line and arc of each kinematic chain's workspace with the workspaces of the other kinematic chains, dividing each line and arc into smaller segments.
3. Determine which of these segments belong to the workspace of the manipulator.
4. Compute the contribution of each line and arc segment in the workspace and add them to obtain the area of the workspace of the manipulator.

Steps 1 through 3 explain the method to determine a geometric representation of the workspace while the fourth step yields a scalar value of the area of the workspace. The first of these steps is explained in [12] and is summarized in the next section where the equations and conditions necessary for the implementation of the method are provided.

Workspace of Each Kinematic Chain [12]

As discussed above, the first step in determining the workspace of planar parallel manipulators is to determine the geometry of the workspace of each kinematic chain. In order to do this for kinematically redundant PRRR kinematic chains, it is necessary to first understand the workspace of their non-redundant RRR kinematic chains from the relatively well known 3-RRR manipulator. Figure 2 shows an example RRR kinematic chain where L_1 and L_2 are, respectively, the lengths of the proximal and distal links, L_3 is the length representing the end-effector platform, (X_1,Y_1) are the coordinates of the fixed base of the RRR kinematic chain, (X_2,Y_2) are the coordinates of the the end-effector for a given posture and L_0 is the distance between (X_1,Y_1) and (X_2,Y_2).

A four-bar mechanism analogy was used to identify three classes of RRR kinematic chains as illustrated in Figure 3 where the concentric circles of each class are associated with one of three radii (r_1, r_2 and r_3) and their definitions are given in the following three equations:

$$\begin{aligned} r_1 &= S + M - L \\ r_2 &= |L_1 - L_2| + L_3 \\ r_3 &= L_1 + L_2 - L_3 \end{aligned} \tag{1}$$

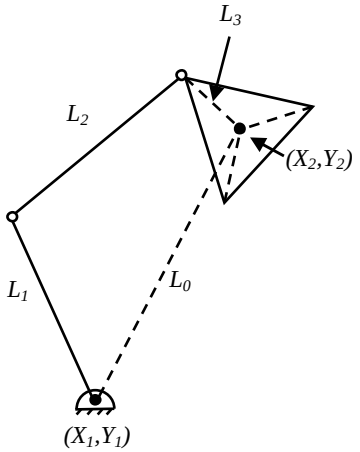

Figure 2. Example RRR kinematic chain

where S is the length of the shortest link, L is the length of the longest link and M is the length of the remaining link.

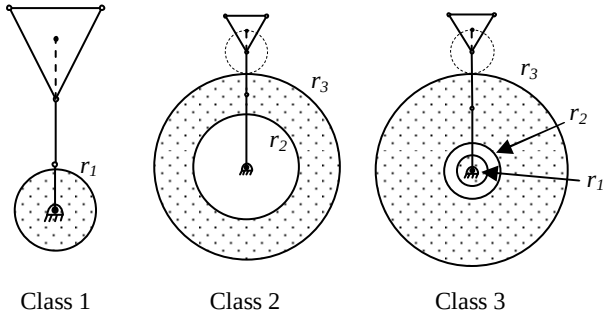

Figure 3. The 3 classes of workspaces of RRR kinematic chains

The basic idea behind the method is that for a given position of the end-effector (X_2, Y_2), the link L_3 must be able to complete a full revolution for the point to be considered inside the workspace. As the end-effector position changes, L_0 (see Figure 2) varies and conditions in which the four-bar mechanism is a double crank, a crank-rocker and a change point, with L_3 as a crank, are determined. The radii r_i, $i = 1,2,3$, represent the limits on L_0 for the different four-bar mechanism categories based on Grashof's criterion. Each class depends on the relationship between the link lengths, and the conditions for each class to exist are summarized in Table 1. These links exclude L_0 as it is dependant on the end-effector position and is not a physical dimension of the kinematic chain.

Adding the effect of the prismatic actuator creates five types of workspaces for the PRRR kinematic chains from the three

Table 1. Conditions for each RRR kinematic chain class

	No link longer than sum of others	**One link longer than sum of others**
L_3 **shortest**	Class 3 (r_1, r_2 and r_3)	Class 2 (r_2 and r_3)
L_3 **not shortest**	Class 1 (r_1)	No workspace

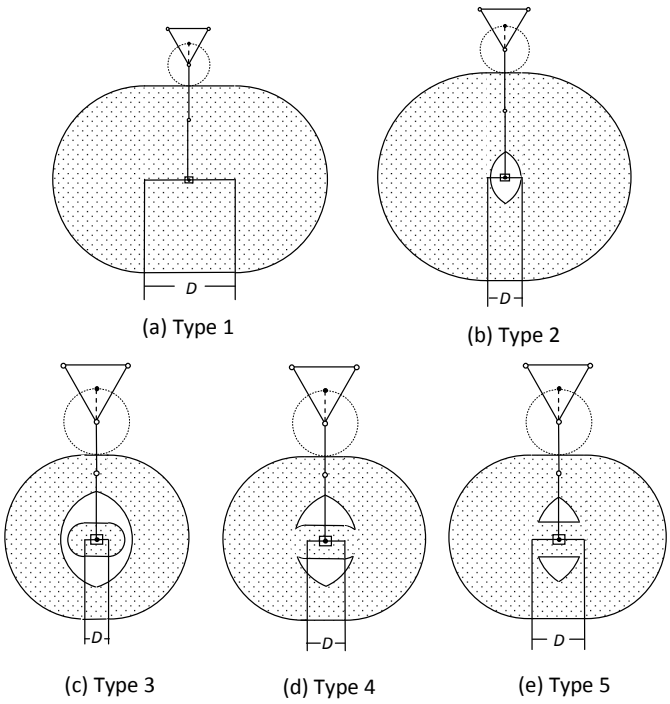

Figure 4. The 5 types of workspaces of PRRR kinematic chains

classes of RRR kinematic chains. These are illustrated in Figure 4 where D is the length of the stroke of the prismatic actuator. In this figure, it can be seen that the prismatic actuator has the effect of stretching the dexterous parts of the workspace defined by r_1 and r_3 while shrinking the inner non-dexterous parts defined by r_2.

Depending on the dimensions of the links (the RRR class and its associated radii), as well as the stroke of the prismatic actuator, a particular PRRR kinematic chain will fall into one of the five types. Types 4 and 5, although similar, differ by the number of arcs and lines needed to define the workspace. The conditions for each type are explained further in [12] and are summarized in Table 2. From this, the geometry of the workspace of each kinematic chain can be defined.

Once the geometry of each kinematic chain is obtained, it

Table 2. Conditions for each type of PRRR workspace

Type	Class	Condition	Figure
	1	$D > 0$	
1	2	$D \geqslant 2r_2$	4(a)
	3	$D \geqslant 2\sqrt{r_2^2 - r_1^2}$	
2	2	$D < 2r_2$	4(b)
3	3	$D < r_2 - r_1$	4(c)
4	3	$r_2 - r_1 \leq D < \sqrt{r_2^2 - r_1^2}$	4(d)
5	3	$\sqrt{r_2^2 - r_1^2} < D \leqslant 2\sqrt{r_2^2 - r_1^2}$	4(e)

is necessary to define each of its arcs and lines. For the planar surfaces dealt with here, a line requires four parameters to define while an arc requires five parameters. Using basic principles of trigonometry, the parameters of the arcs and lines of each kinematic chain can readily be defined.

Boundary Determination of n-PRRR Planar Parallel Manipulators

In this section, the geometry of the workspace of n-PRRR manipulators is determined. This refers to steps 2 and 3 of the method presented. When the PRRR kinematic chains are assembled to create an n-PRRR manipulator, the workspace consists of the intersection of the workspaces of all kinematic chains.

Step 2 of the method consists of finding all the points of intersection between all the lines and arcs of the workspace of every kinematic chain and the lines and arcs of the workspace of the other kinematic chains. The points of intersection of two arcs, two lines and an arc and a line can easily be determined.

Once all points of intersection for a particular arc or line are determined, that arc or line can be segmented into shorter arcs and lines. These are, henceforth, simply called segments. Let A be the arc or line to be segmented and a_i be the segments of A, where $i = 1...N+1$, where N is the number of intersections of A. In order to segment A, its points of intersection are sorted from the closest to the beginning of A to the end of A. Thus, a_1 is the segment from the beginning of A to the first point of intersection, a_j with $j = 2...N$ is the segment from the $(j-1)$th point of intersection to the jth point of intersection and a_{N+1} is the segment from the last point of intersection to the end of A. After the segmentation of each arc and line is done, a complete list of segments is generated and the second step in the method is complete.

The third and last step in the determination of the boundary of the workspace of n-PRRR manipulators consists of determining which segments described above are parts of the boundary. The following two facts simplify the process to determine the workspace of planar n-PRRR manipulators.

1. Any segment that is inside the workspace of every kinematic chain from which it does not originate is a part of the boundary of the workspace of the manipulator.
2. If one point on the segment is inside the workspace, the entire segment is included.

The effort of determining if a segment is included in the workspace is thus reduced to checking whether a point on the segment is in the workspace. The mid-point is usually used for this purpose as it is easily identified and is further from the edges to avoid potential errors due to the truncation of the computational variables.

The workspace boundary for all the five types of workspaces are composed of up to three regions that can have one of two basic shapes. Figure 5(a) illustrates these regions on an example workspace of Type 5. Each of these regions are defined by one of the three radii defined in Equation (1) and by the stroke of the prismatic actuator.

The workspace regions defined by r_1 and r_3 are of similar shape composed of the union of two circles of radii r_1 or r_3 and a rectangle where the width is equal to the stroke of the prismatic actuator (D). This is shown in Figure 5(b). The workspace region defined by r_2 is simply the intersection of two circles of radii r_2 as shown in Figure 5(c) and represents a void in the workspace.

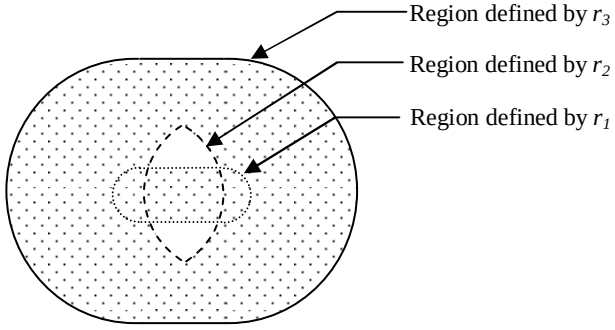

(a) Regions of the workspace

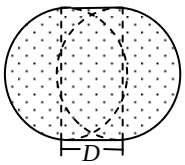

(b) Region defined by r_1 or r_3

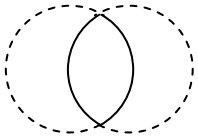

(c) Region defined by r_2

Figure 5. Shapes of regions of the workspace of a PRRR kinematic chain

A point is in a workspace region defined by r_1 or r_3 if it is

inside one of the two circles or the rectangle, while it is included in a workspace region defined by r_2 if it is inside its two circles simultaneously.

The procedure to determine whether a point on an arc or line segment is inside the workspace of a kinematic chain differs depending on the type of workspace of the kinematic chain. If the chain's workspace is of Type 3, 4 or 5, the process is summarized by the following:

1. Determine if the point is in the workspace region defined by r_3. If yes, go to step 2. If no, stop: the point is not included in the workspace of the kinematic chain.
2. Determine if the point is in the workspace region defined by r_2. If yes, go to step 3. If no, stop: the point is included in the workspace of the kinematic chain.
3. Determine if the point is in the workspace region defined by r_1. If yes, the point is included in the workspace of the kinematic chain. If no, the point is not included in the workspace of the kinematic chain.

If the kinematic chain's workspace is of Type 2, the process is summarized by the following:

1. Determine if the point is in the workspace region defined by r_3. If yes, go to step 2. If no, stop: the point is not included in the workspace of the kinematic chain.
2. Determine if the point is in the workspace region defined by r_2. If yes, the point is not included in the workspace of the kinematic chain. If no, the point is included in the workspace of the kinematic chain.

Finally, if the workspace is of Type 1, the only region present is defined by either r_1 or r_3 where the point is included in the workspace of the kinematic chain if it is inside that region. An algorithm was developed to implement the method, however it was too lengthy to include in the paper. A code for the fully automatic determination of the n-PRRR workspace was written in MATLAB®.

Workspace Area of n-PRRR Planar Parallel Manipulators

An integration on the boundary can be done to compute the workspace area. The Gauss Divergence Theorem [9] can be applied to planar surfaces yielding:

$$A = \frac{1}{2}\int_{\partial\Omega} \mathbf{s}^T \mathbf{n} d\partial\Omega \tag{2}$$

where A is the area of the surface, $\partial\Omega$ is the boundary of the surface, $\mathbf{s}$ is the position vector of a point on the boundary and $\mathbf{n}$ is the unit vector, normal to and outward from the boundary.

Equation (2) can be rewritten as a series of sums as:

$$A = \frac{1}{2}\left(\sum_{i=1}^{Na} A_i + \sum_{i=1}^{N_l} B_i\right) \tag{3}$$

where

$$A_i = \int_{\partial\Omega_i^a} \mathbf{s}^T \mathbf{n} \mathrm{d}\partial\Omega_i^a \tag{4}$$

$$B_i = \int_{\partial\Omega_i^l} \mathbf{s}^T \mathbf{n} \mathrm{d}\partial\Omega_i^l \tag{5}$$

where N_a and N_l are the number of arc and line segments on the boundary, respectively, and where $\partial\Omega_i^a$ and $\partial\Omega_i^l$ are the ith arc segment and the ith line segment, respectively. This method has the advantage that the boundary segments are not required to be in any particular order. The contribution of each is calculated separately and simply added as per Equation (3) to yield the workspace area. Furthermore, simple closed-form expressions for A_i can be obtained [7]:

$$A_i = ar[\sin\theta_{max} - \sin\theta_{min}] - br[\cos\theta_{max} - \cos\theta_{min}] + r^2[\theta_{max} - \theta_{min}] \tag{6}$$

for an outer arc and

$$A_i = -ar[\sin\theta_{max} - \sin\theta_{min}] + br[\cos\theta_{max} - \cos\theta_{min}] - r^2[\theta_{max} - \theta_{min}] \tag{7}$$

for an inner arc, where (a,b) are the coordinates of the center of the circle from which the arc originates, r is the radius and θ_{min} and θ_{max} are the angles of the beginning and the end of the arc, respectively. For the present case, an arc of radius $r_1$or r_3 is an outer arc and thus uses Equation (6), and an arc of radius r_2 is an inner arc using Equation (7). Closed-form expressions can also be obtained for B_i (adapted from [7]):

$$B_i = L(x_{1i}\sin\theta_i - y_{1i}\cos\theta_i) \tag{8}$$

and

$$B_i = L(-x_{1i}\sin\theta_i + y_{1i}\cos\theta_i) \tag{9}$$

where (x_{1i},y_{1i}) are the coordinates of the beginning of the line segment, L is its length and θ_i is the angle of the orientation of the line toward its end point. If the point is chosen as the beginning point of the line such that $x_{1i} \leq x_{2i}$, where x_{2i} is the x coordinate of the end point of the line segment, then θ_i will always be bounded by $-\frac{\pi}{2} \leq \theta_i \leq \frac{\pi}{2}$ rad. Thus, equation (8) is used when the workspace is above the line as illustrated by Figure 6(a). Equation (9) is used when the workspace is below the line as illustrated by Figure 6(b). Note that $x_{1i} = x_{2i}$ is a particular case when the line is vertical where Equation (8) is used when the workspace is on the left of the line and Equation (9) is used when the workspace is on its right. Also note that when $x_{1i} = x_{2i}$, the beginning point of the line must be used such that $y_{1i} < y_{2i}$.

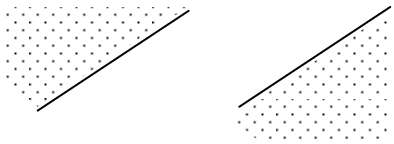

(a) (b)

Figure 6. Example line segments as part of the workspace boundary

EXAMPLE n-PRRR MANIPULATORS

In order to demonstrate applications of the method, two example n-PRRR manipulators are presented in this section. The first manipulator is a 3-PRRR manipulator, shown in Figure 7. In this figure, the dotted lines indicate the strokes of the prismatic actuators.

The dimensions of each kinematic chain of this manipulator are shown in Table 3 where (X_i^{min},Y_i^{min}) and (X_i^{max},Y_i^{max}) are, respectively, the coordinates of the minimum and maximum limits of the prismatic actuator of the ith kinematic chain as seen in Figure 7. With these dimensions, each kinematic chain has a Type 2 workspace.

The boundary and the area A of the workspace of the 3-PRRR manipulator described above are shown in Figure 8.

Since the workspace boundary of every kinematic chain is determined individually, the stroke of the prismatic actuators can be configured in any orientation and any number of kinematic chains can be used. Figure 9 illustrates an example manipulator with four kinematic chains and with the prismatic actuators configured in arbitrary orientations. Table 4 shows the dimensions of this manipulator and Figure 10 illustrates the workspace boundary as well as its total area A. For this manipulator, each kinematic chain has a Type 2 workspace except for the third one, who has a Type 1 workspace.

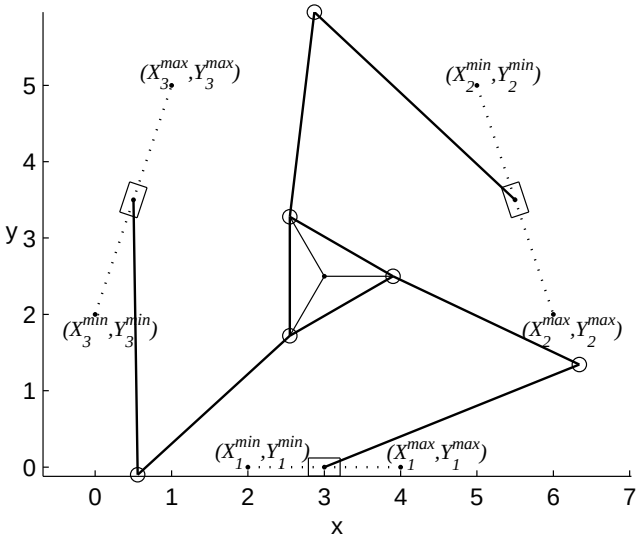

Figure 7. Example 3-PRRR manipulator

Table 3. Dimensions of the example 3-PRRR manipulator

	Kinematic chain		
	1	2	3
L_1	3.6	3.6	3.6
L_2	2.7	2.7	2.7
L_3	0.9	0.9	0.9
(X_i^{min},Y_i^{min})	(2,0)	(5,5)	(0,2)
(X_i^{max},Y_i^{max})	(4,0)	(6,2)	(1,5)

Table 4. Dimensions of the example 4-PRRR manipulator

	Kinematic chain			
	1	2	3	4
L_1	3.6	2.7	3	1.7
L_2	2.7	3.6	3	2.9
L_3	0.9	0.7	0.9	1.1
(X_i^{min},Y_i^{min})	(-3,-3)	(1,-1)	(1,1)	(-2.5,0.8)
(X_i^{max},Y_i^{max})	(-1,-1)	(3,-2.5)	(1,4)	(0,0.8)

CONCLUSION

A method designed to determine the geometry and the total area of the dexterous workspace for kinematically redundant n-PRRR planar architectures has been presented in this paper. First, an explanation of the dexterous workspace of each kine-

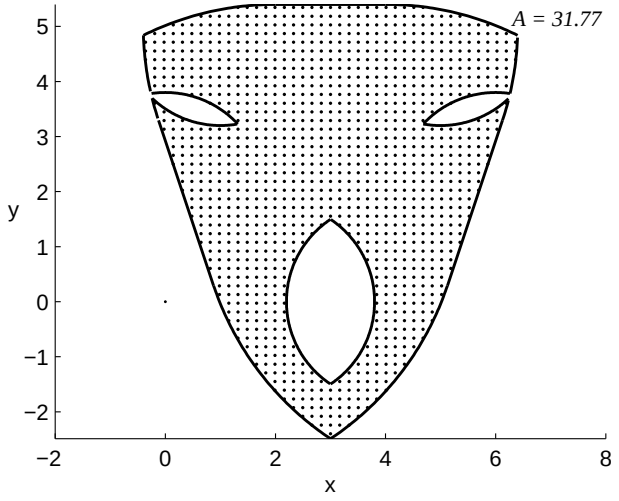

Figure 8. Example 3-PRRR manipulator workspace

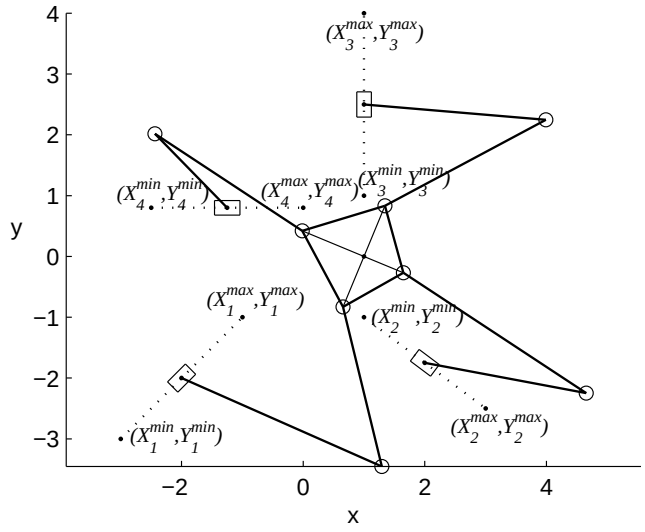

Figure 9. Example 4-PRRR manipulator

matic chain was given. Then, a method to determine the boundary of the intersection of the workspaces of all the kinematic chains was presented to obtain the manipulator's workspace. Finally, the Gauss Divergence Theorem was employed to yield the total area of the dexterous workspace of any n-PRRR manipulator. The dexterous workspaces of two example n-PRRR manipulators were also given to demonstrate the method. With these examples, it was seen that voids in the manipulator's workspace were readily detected.

The dexterous workspace of manipulators is an important criterion for their design. The implementation of this method is a useful tool in the design of kinematically redundant planar

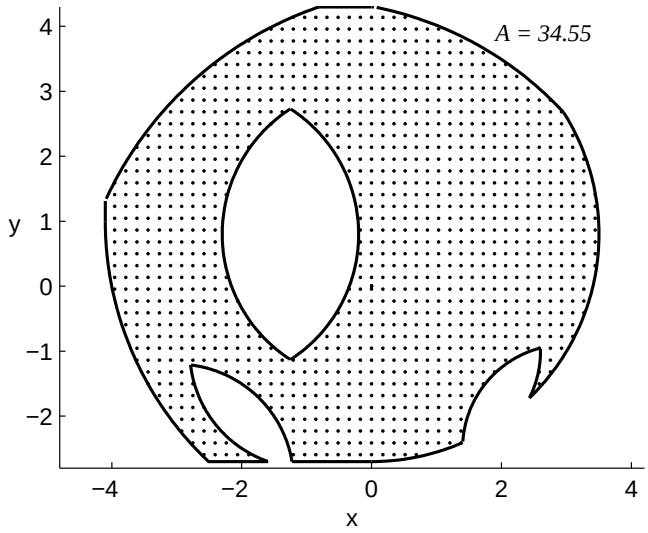

Figure 10. Example 4-PRRR manipulator workspace

parallel manipulators. Many parts of this method can also be applied to kinematically redundant planar parallel manipulators of architectures other than n-PRRR. Since the method is based on an analogy with the four-bar mechanism, it cannot be extended to spacial mechanisms.

ACKNOWLEDGMENT

The authors would like to thank the Natural Sciences and Engineering Research Council of Canada (NSERC) for its support in funding this research.

REFERENCES

[1] Gosselin, C., and Angeles, J., 1988. "The optimum kinematic design of a planar three-degree-of-freedom parallel manipulator". *ASME Journal of Mechanisms, Transmissions and Automation in Design,* ***110***(1), pp. 35–41.

[2] Williams II, R. L., and Reinholtz, C. F., 1988. "Closed-form workspace determination and optimization for parallel robot mechanisms". In ASME Design Technology Conferences 20th Biennial Mechanisms Conf., pp. 341–351.

[3] Kumar, V., 1992. "Characterization of workspaces of parallel manipulators". *ASME Journal of Mechanical Design,* ***114***(3), pp. 368–375.

[4] Pennock, G. R., and Kassner, D. J., 1993. "The workspace of a general geometry planar three-degree-of-freedom platform-type manipulator". *ASME Journal of Mechanical Design,* ***115***(2), pp. 269–276.

[5] Merlet, J.-P., Gosselin, C., and Mouly, N., 1998.

"Workspaces of planar parallel manipulators". *Mechanisms and Machine Theory,* ***33***(1-2), pp. 7–20.

[6] Zhaohui, L., and Zhonghe, Y., 2004. "Determination of dexterous workspace of planar 3-dof parallel manipulator by auxiliary linkages". *Chinese Journal of Mechanical Engineering (English edition),* ***17***((Suppl.)), pp. 76–78.

[7] Gosselin, C., and Jean, M., 1996. "Determination of the workspace of planar parallel manipulators with joint limits". *Robotics and Autonomous Systems,* ***17***(1996), pp. 129–138.

[8] Hay, A. M., and Snyman, J. A., 2002. "The chord method for the determination of nonconvex workspaces of planar parallel manipulators". *Computers and Mathematics with Applications,* ***43***, pp. 1135–1151.

[9] Buck, R. C., 1965. *Advanced Calculus*, 2 ed. International series in pure and applied mathematics. McGraw-Hill Book Company.

[10] Gosselin, C., 1990. "Determination of the workspace of 6-dof parallel manipulators". *ASME Journal of Mechanical Design,* ***112***(3), pp. 331–336.

[11] Ebrahimi, I., Carretero, J. A., and Boudreau, R., 2008. "A family of kinematically redundant planar parallel manipulators". *ASME Journal of Mechanical Design,* ***130***(6), pp. 062306–1– 062306–8.

[12] Gallant, A., Boudreau, R., and Gallant, M., 2009. "Dexterous workspace of a 3-PRRR kinematically redundant planar parallel manipulator". *Transactions of the CSME,* ***33***(4), pp. 645–654.